NO ($v'' = 0$) Rotational Distributions from the Photodissociation of Organometallic Nitrosyls in the Charge Transfer Region

Jeffrey A. Bartz,[†,*] Shino Odawara,[‡,§] Sarah A. Collier,[†] Karl M. Meisel,[†] Kevin P. Burke,[†] James J. Cekola,[†] and George E. Leroi[‡]

Department of Chemistry, Kalamazoo College, 1200 Academy Street, Kalamazoo, Michigan 49006-3295, and Department of Chemistry and LASER Laboratory, Michigan State University, East Lansing, Michigan 48824-1322

Received: September 15, 2000; In Final Form: November 16, 2000

The photodissociations of two metal nitrosyl compounds, $Co(CO)_3NO$ and $Mn(CO)_4NO$, were studied at 450 nm, in the metal-to-nitrosyl charge-transfer region for both compounds. The rotational distributions of free NO in the $v'' = 0$ vibrational state were determined by laser-induced fluorescence excitation. A Surprisal Analysis shows that the NO population distributions display a dynamical bias toward lower rotation in both compounds. The similarity between the NO rotational distributions is surprising, considering that $Co(CO)_3NO$ was expected to dissociate through a bent transition state and $Mn(CO)_4NO$ was not. The spin−orbit populations of the NO products ($^2\Pi_{1/2}$ and $^2\Pi_{3/2}$) are equally populated in both compounds, indicating that the electronic surfaces that produce these two states are strongly coupled at the transition state. An upper limit of the M−NO bond dissociation energy is estimated at 52 kcal/mol from the rotational assignments.

I. Introduction

Gas-phase organometallic photochemistry is important for understanding the formation and behavior of coordinatively unsaturated organometallic species that play important roles in vapor deposition processes and catalysis. For example, $Co(CO)_3NO$ has been used to form thin films of cobalt and cobalt oxonitride by chemical vapor deposition.[1,2] Metal nitrosyl compounds are of particular interest because of the role of metallonitrosyl biological systems.[3] This contribution investigates the role of doubly degenerate excited states in the dissociation of volatile organometallic nitrosyl compounds.

Gas-phase molecules of the form R−NO have been studied by laser excitation methods.[4−14] Depending on the R group and the excitation energy, the NO fragments can display statistical or nonstatistical behavior in the NO rotational distribution as well as in the two spin−orbit states of the free NO. In organic nitrite and nitroso compounds the terminal NO is bound to the neighboring atom with a bond angle of 120° or less. The initial geometry suggests that dissociation of the NO fragment should occur through a bent transition state and that the dissociated NO should generally have a high degree of rotation, which is seen in many compounds.[5,6,13,15] The initial geometries and photodissociation behavior of the organometallic nitrosyls are more complex because of the participation of d orbitals.

Condensed phase photochemistry studies of organometallic nitrosyls have shown that a metal-to-nitrosyl charge transfer forms a long-lived charge transfer state. Crichton and Rest reported that photolysis of $Co(CO)_3NO$ in a cryogenic matrix formed $Co(CO)_2NO$; however, substitution reactions also indicated that the parent molecule undergoes nucleophilic attack, presumed to initiate through a metal-to-nitrosyl charge transfer.[16] Keeton and Basolo reported similar associative photochemical pathways for solution phase photochemical substitution in $Mn(CO)_4NO$.[17] Crichton and Rest also investigated the primary photolysis products of $Mn(CO)_4NO$ in a frozen gas matrix and found both carbonyl loss and evidence for a metal-to-nitrosyl charge transfer by observing a low value of ν(NO) at 1460 cm^{-1}, as compared to the ν(NO) in the parent molecule of 1770 cm^{-1}.[18] Chen et al. have shown that excitation of η^5-CpNiNO in the metal-to-ligand charge transfer (MLCT) region not only decreases the NO stretching frequency from 1824 to 1387 cm^{-1} but also bends the Ni−NO bond, as determined by EXAFS.[19] In the gas phase, excitation of organometallic nitrosyls in the MLCT region is believed to form a bent M−NO bond. Evans and Zink studied the photochemical behavior of $Co(CO)_3NO$ and interpreted gas-phase photochemical reactions of $Co(CO)_3NO$ in terms of a bent Co−NO transition state arising from a Jahn−Teller distortion of the excited state.[20] Further gas-phase photodissociation experiments of metal nitrosyl compounds were reported by Georgiou and Wight, who monitored free NO by resonance-enhanced multiphoton ionization (REMPI). They found that the calculated rotational distributions of NO that agreed best with the experimental data from the 450 nm photodissociation of $Co(CO)_3NO$ and η^5-CpNiNO were peaked at high J'' values, indicating impulsive dissociation through a bent transition state.[21,22]

In the ground states of both $Co(CO)_3NO$ (**1**) and $Mn(CO)_4NO$ (**2**), the metal−NO bond is linear. By simple electron counting arguments, a linear NO is considered formally NO^+, isoelec-

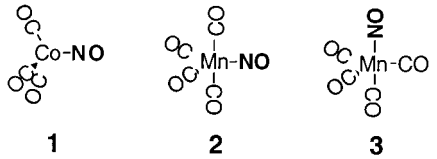

1 **2** **3**

* Author to whom correspondence should be addressed. E-mail: jbartz@kzoo.edu. Fax: (616) 337-7251.
† Kalamazoo College.
‡ Michigan State University.
§ Current address: Nihon University, Department of Industrial Chemistry, College of Engineering, Koriyama, Japan.

10.1021/jp003293r CCC: $20.00
Published on Web 01/11/2001

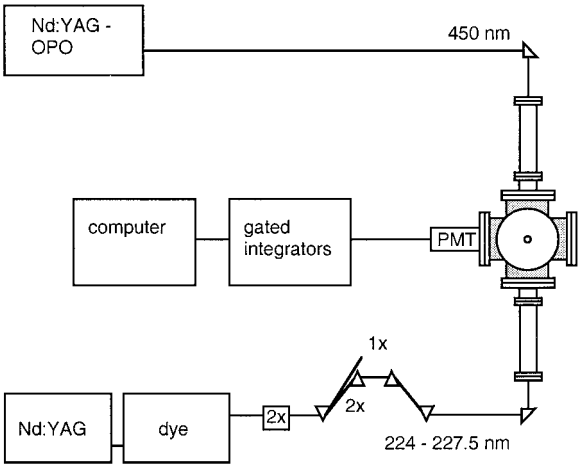

Figure 1. Experimental layout for the two-color 450 nm pump and UV (224−227.5 nm) probe experiments.

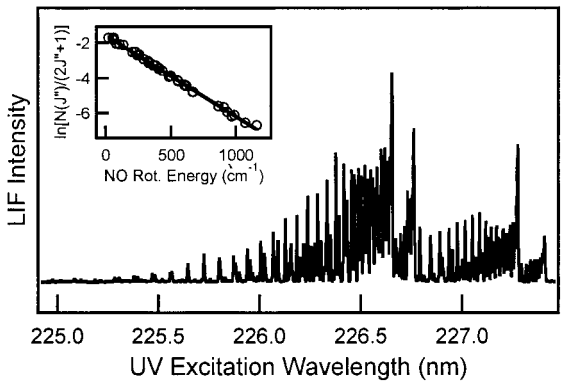

Figure 2. One photon UV laser-induced fluorescence excitation spectrum of room-temperature NO in the region 224.9−227.5 nm. The inset is a Boltzmann plot of the rotational state distribution extracted from the laser-induced fluorescence data. The temperature determined from the linear least-squares fit to the points is 303 ± 11 K.

tronic with CO, but participating in a three electron donation to the metal center. In either $Mn(CO)_4NO$ or $Co(CO)_3NO$, absorption of a 450 nm photon excites the molecules in a well-resolved feature in the visible and near-UV region of the UV−vis absorption spectrum. This transition is assigned as a metal-to-ligand charge transfer, from a molecular orbital of primarily d_{z^2} character to a molecular orbital of primarily NO π^* antibonding character.[23] In C_{3v} $Co(CO)_3NO$, populating the π^*(NO) occupies one of two doubly degenerate orbitals, which would lead to a Jahn−Teller distortion to remove the degeneracy of the inequivalent orbitals. In C_{2v} $Mn(CO)_4NO$, the MLCT transition populates a nondegenerate state, which would not be expected to undergo the Jahn−Teller distortion. Herein we report on the gas-phase photodissociation of $Co(CO)_3NO$ and $Mn(CO)_4NO$ at 450 nm to investigate the similarities and differences in the dynamical behavior and to determine the role of doubly degenerate orbitals in the dynamical behavior.

II. Experimental Section

$Co(CO)_3NO$ was purchased from Strem Chemical or was synthesized by the method of Job and Rovang.[24] $Mn(CO)_4NO$ was synthesized by the method of Treichel et al.[25] Samples were stored in a 0 °C freezer and purified by several freeze−pump−thaw cycles prior to use. FTIR spectra were taken to monitor the purity of the samples and for free NO. NO (AGA) was used without further purification.

The experimental layout appears schematically in Figure 1. The neat organometallic sample was introduced into the vacuum chamber through a solenoid valve (General Valve Series 9) with a 0.049 in. orifice. A home-built nozzle driver provided the 160 μs, 200 V pulse to the solenoid valve. The vacuum chamber was pumped by a diffusion pump (Varian VHS-6), backed by a 17 L/s roughing pump (Alcatel 2020A).

In all experiments, the 224−227.5 nm UV light was produced by a Nd:YAG laser (Quanta-Ray DCR-2) that pumped a dye laser (Quanta-Ray PDL-1.) The dye output was doubled in a BBO crystal (Inrad). The harmonic was separated from the fundamental by a series of four 60° quartz prisms and resulted in 50−100 μJ of doubled output. The ca. 10 ns pulses of laser light were approximately 3 mm in diameter and remained unfocused in these experiments. The energy density was approximately 0.7−1.4 mJ/cm^2. The laser power was monitored with a pyroelectric detector (Molectron J8LP). The output of the pyroelectric detector was averaged with a gated integrator (Stanford Research Systems 250).

In these two-color experiments, the 450 nm pump beam was produced by a Nd:YAG-pumped OPO laser system (Coherent Infinity/XPO). The ca. 10 ns pulses of laser light had energies of 5−10 mJ/pulse, as monitored by a photodiode, and were approximately 5 mm in diameter. The 450 nm pump beam was unfocused in these experiments, giving an energy density of approximately 25−50 mJ/cm^2. The typical delay between the pump and probe lasers was 100 ns and was controlled by a digital delay generator (Stanford DG535).

Laser-induced fluorescence was monitored with a PMT (Hamamatsu 924B) situated at right angles to both the laser and molecular beam axes. A 30 nm band-pass filter (Janos XB02) and a UG-5 filter were used to remove spontaneous fluorescence from metal atoms and scattered laser light. The emission signal was monitored on an oscilloscope (Tektronix TDS620B). The induced NO fluorescence signal was averaged with a gated integrator (Stanford Research Systems SR250), digitized (National Instruments DAQ-1200), and stored on a laptop computer. The gate widths were typically 200 ns and delayed 120 ns after the probe laser pulse. Additional gated integrators averaged the output of the laser energy monitors, which were digitized and stored along with the signals.

III. Results

Laser-induced fluorescence (LIF) excitation was performed on a static bulb of pure NO to validate the method for data collection and data analysis. The LIF spectrum of room-temperature NO appears in Figure 2. Individual NO transitions were assigned with the help of published spectroscopic parameters.[26] The inset in Figure 2 is the Boltzmann plot of the pure NO data, where the log of the intensity of each of the assigned lines divided by the appropriate Hönl-London factor[27] is plotted versus the rotational energy of each state. The intensities of the individual features were normalized by the laser power. In the inset in Figure 2, four sets of transitions ($Q_{11} + P_{21}$, $Q_{21} + R_{11}$, $Q_{12} + P_{22}$, and $Q_{22} + R_{12}$) are overlaid. The points corresponding to the latter two sets of transitions were adjusted to account for the energy difference between the $^2\Pi_{1/2}$ and $^2\Pi_{3/2}$ electronic states; 121 cm^{-1} was added to the rotational energy for the transitions from the upper electronic state. There are too few individual transitions assigned from the other branches (P_{11}, R_{21}, P_{12}, R_{22}), because of spectral congestion, to make meaningful plots from those data. A line fitted to the points in the Figure 2 inset is inversely proportional to the Boltzmann rotational temperature, which in this case is 303 ± 11 K. Each of the

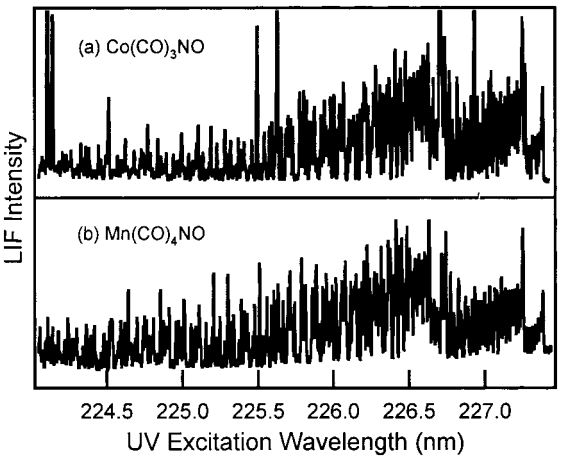

Figure 3. Laser-induced fluorescence excitation of the nascent NO photoproduct from the 450 nm photodissociation of (a) $Co(CO)_3NO$ and (b) $Mn(CO)_4NO$.

pairs of transitions gives the same Boltzmann temperature, within the error of the fits of the four sets of transitions.

Figure 3a is the LIF spectrum of free NO following the 450 nm photodissociation of $Co(CO)_3NO$; Figure 3b shows the corresponding spectrum for $Mn(CO)_4NO$. In Figure 3a there are several features due to the UV laser-induced fluorescence of Co atoms produced in the multiphoton dissociation of the parent compound. Contributions from many of the fast emitting Co* emission lines are minimized by the 120 ns gate delay. Additional Co* emission features were identified by their intensity and position and not included in the NO laser-induced fluorescence excitation data analysis.

In conducting this two-color photodissociation/LIF experiment, it is important to consider the effect of any one-color UV photodissociation/LIF in the observed signal. Such one-color photodissociation and detection in organometallic nitrosyls has been used by us and others to detect free NO in the course of a single UV laser pulse.[28−30] To remove the effect of one-color photodissociation/LIF, the gated integrator/boxcar averager was operated in the active background subtraction mode. The 450 nm photolysis laser was pulsed at 5 Hz and the UV probe laser pulsed at twice the rate, 10 Hz. Between each 450 nm pump/UV probe event, in which the UV probe pulse was delayed from the 450 nm pump pulse by 100 ns, a UV laser pulse went through the sample alone. Any NO LIF signal detected from only the UV pulse was treated as background and was subtracted from the two-color signal.

To test the active background subtraction method of data collection, two experiments were run. In the first experiment, both the 450 nm pump laser and the UV probe laser passed through the molecular beam. The difference between the 450 nm pump/UV probe signal and the delayed UV-only background gives the contribution from the 450 nm pump/UV probe experiment. In the second experiment the 450 nm pump laser was blocked and only the UV probe laser was allowed to pass through the sample. The gated integrator/boxcar averager still subtracted every other probe pulse from the "signal," here the LIF from a UV-only pump/probe signal. The difference between the two UV-only events should be zero. The results from the two experiments appear in Figure 4. For each data point in the LIF spectra in Figure 4, fifteen signal minus background events were averaged. With both lasers illuminating the sample and the integrators actively subtracting every other laser pulse event, the signal appears (solid line), but with solely the probe laser present, only baseline appears (dotted line). In addition, the PMT does not detect any NO LIF signal when the UV probe beam is blocked.

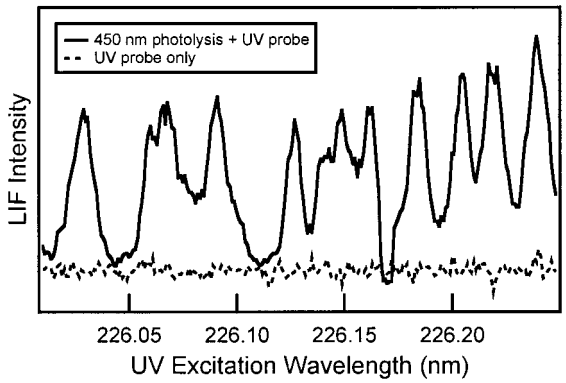

Figure 4. Single photon UV laser-induced fluorescence excitation of NO following the photodissociation of $Mn(CO)_4NO$ at 450 nm (solid line) and the UV laser alone (dashed line).

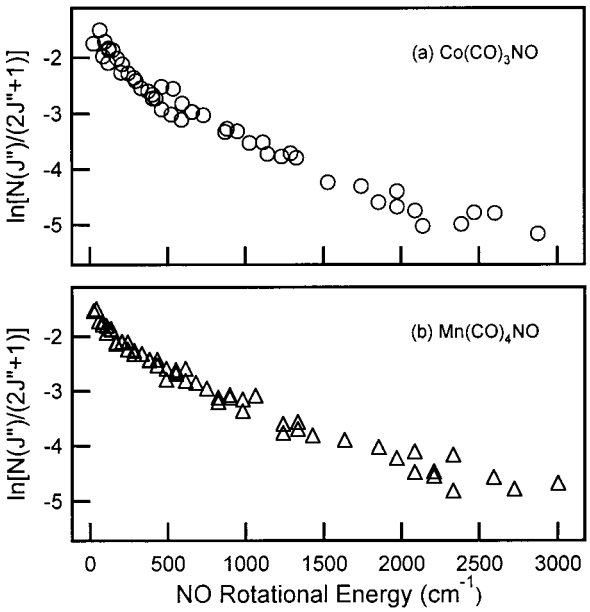

Figure 5. Boltzmann plot of the NO rotational distribution following the 450 nm photodissociation of (a) $Co(CO)_3NO$ and (b) $Mn(CO)_4NO$ as detected by laser-induced fluorescence excitation.

Power dependences of the NO fluorescence signal for the 450 nm pump beam as well as the UV probe beam were determined for both $Co(CO)_3NO$ and $Mn(CO)_4NO$. The power dependence of the NO signal is 1.0 ± 0.1 for both the 450 nm pump laser and the UV probe laser for both compounds.

Figure 5 contains Boltzmann plots of the NO populations following the 450 nm photodissociation of (a) $Co(CO)_3NO$ and (b) $Mn(CO)_4NO$.

IV. Discussion

The photodissociations of both $Co(CO)_3NO$ and $Mn(CO)_4NO$ to produce free NO appear to be one photon processes according to the power dependences. It is evident in Figure 3a that multiphoton dissociation is also occurring in the photolysis of $Co(CO)_3NO$ because of the appearance of Co atoms, a process that would take at least three 450 nm photons. This raises a concern that this 450 nm experiment may be a coherent two-photon process, energetically equivalent to a 225 nm photodissociation experiment. In both molecules, however, the NO rotational distributions in the one-color UV-only pump−probe

experiments[28,31] and the 450 nm pump/UV probe experiments have different population distributions. In a comparison of the 450 nm photolysis data to the 225 nm photolysis data, the rotational distributions show a significantly larger population at higher J'' at the higher 225 nm photon energy. This indicates that the rotational population arises from higher available energies in the 225 nm case and also may indicate that the pathways and intermediates involved in producing NO at the two wavelengths are different.

Several conclusions can be drawn from the Boltzmann plots in Figure 5. First, the $^2\Pi_{1/2}$ and $^2\Pi_{3/2}$ electronic states, which differ in energy by 121 cm^{-1}, are equally populated. This is evident by the absence of two separate distributions, due to the two electronic states of NO, in the Boltzmann plots. Quantitative comparisons of the individual transitions in NO produced from both compounds were also made and resulted in a F_1/F_2 ($^2\Pi_{1/2}/^2\Pi_{3/2}$) ratio of 1.0 for both compounds. The absence of any difference in the two populations reveals that the coupling of the electronic surfaces leading to NO in the $^2\Pi_{1/2}$ or $^2\Pi_{3/2}$ states is strong enough that the molecule exiting the transition state has no memory of the initial excited state. Moreover, at the transition state the dissociating molecule does not feel the effect of the 121 cm^{-1} energy difference in the two separated products. Similar F_1/F_2 ratios have been observed in other large R−NO molecules with sufficient excitation energy, such as *t*-BuNO,[14] but it contrasts with the behavior of smaller molecules, such as CH_3ONO. In the latter the F_1/F_2 ratio is as high as 2 at higher J''.[10]

Second, it is evident in Figure 5 that a Boltzmann distribution is not the best model for describing the energy partitioning into the NO rotational states. The data are not well fit by a line, corresponding to a Boltzmann temperature, because of energetic considerations. The energy difference between a 450 nm photon, with 63 kcal/mol, and the dissociation energy of the M−NO bond leaves little energy to partition into product states. In $Co(CO)_3NO$, the M−NO bond dissociation energy (BDE) has been estimated between 57.5 and 86.4 kcal/mol.[32] The upper limit for the M−NO bond dissociation energy can be estimated here from the data in Figure 3. Because some of the nascent NO fragments are in the $v'' = 1$ vibrational state, the spectral window in which NO ($v'' = 0$) rotational states can be assigned unambiguously starts at the $X(v'' = 0) \rightarrow A(v' = 0)$ bandhead and ends at the $X(v'' = 1) \rightarrow A(v' = 1)$ bandhead. Within this window, the peak that is assigned to a $X(v'' = 0) \rightarrow A(v' = 0)$ transition with the highest internal energy in Figure 3 is $Q_{12}(41.5)$, having a lower state energy of 3845 cm^{-1}. The difference between the photon energy and the energy of $NO(^2P_{3/2})$ in $J'' = 41.5$ provides an upper estimate of the metal BDE at 52 kcal/mol. With a 52 kcal/mol M−NO BDE, only 11 kcal/mol is available to partition into the remaining products, neglecting any initial internal energy in the parent molecule. With little excess energy, a better way to describe the energy partitioning into the product states is to consider how the dissociation event populates phase space through Surprisal Analysis and the Prior Distribution.

The Prior Distribution has been described elsewhere.[33] Briefly, the Prior Distribution accounts for the statistical population of the energy-allowed product states. In the case of energy disposal into rotational states, the Prior Distribution is

$$P^\circ(J'') = (2J'' + 1)(E_{photon} - E_{vib})^{1/2} \qquad (1)$$

where $P^\circ(J'')$ is the Prior Distribution, J'' is the rotational quantum number of NO, E_{photon} is the energy of the photon, and E_{vib} is energy in the $v'' = 0$ vibration. The first term is the degeneracy of the rotational state. The second term accounts for the translational energy density of states. This analysis neglects any energetic contributions from or energy partitioning into the metal-containing fragments. Deviation of the actual experimental NO rotational distribution from the predicted Prior Distribution is determined through a Surprisal Analysis, which measures the deviation through the equation

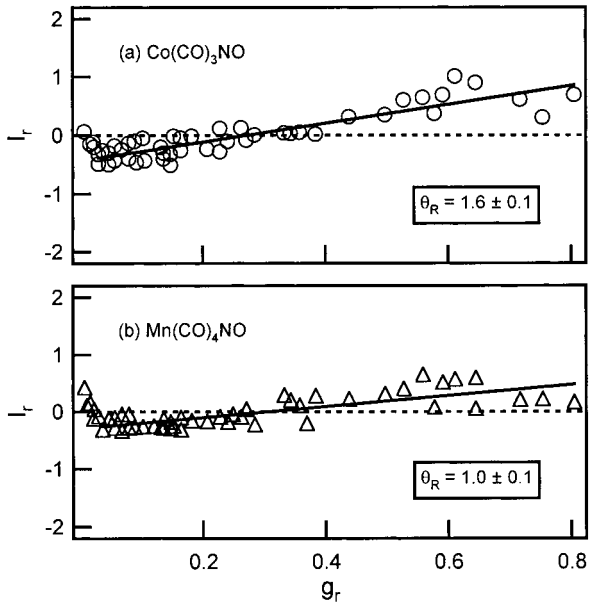

Figure 6. Surprisal Analysis of the NO rotational distribution following the 450 nm photodissociation of (a) $Co(CO)_3NO$ and (b) $Mn(CO)_4NO$ as detected by UV laser-induced fluorescence excitation.

$$I_r = -\ln(P/P^\circ) \qquad (2)$$

where I_r is the Surprisal, P is the experimental distribution, and P° is the Prior Distribution.

Figure 6 is a plot of the Surprisal, I_r, versus the fraction of available energy in rotation, g_r, for (a) $Co(CO)_3NO$ and (b) $Mn(CO)_4NO$. The metal−NO bond dissociation energies were assumed to be 50 kcal/mol in each compound, but in both figures the qualitative appearance of the Surprisal plot did not change if the metal−NO bond dissociation energy was lowered to 40 kcal/mol. In Figure 6 there are linear deviations in the Surprisal plots, indicating a dynamical bias in forming the rotational distributions. The extent of the bias is determined by the slope, labeled θ_R on each plot. The experimental population is cooler than predicted by the Prior Distribution, revealing a dynamical bias away from high rotation in the NO photoproduct and toward low rotation. Moreover, the dynamical bias is higher for $Co(CO)_3NO$, which generates an NO population that is cooler than the distribution from $Mn(CO)_4NO$. The difference in the rotational population distributions can be explained by rapid dissociation and differences in bond dissociation energies between Co−NO and Mn−NO.

It is evident in the Surprisal plots in Figure 6 and from the Boltzmann plots in Figure 5 that $Mn(CO)_4NO$ releases NO with a higher proportion of the population in higher J'' states as compared to $Co(CO)_3NO$, which can be explained by bond dissociation energy differences after a prompt dissociation. Georgiou and Wight photodissociated a series of $Co(CO)_2NOL$ compounds (L = CO or PR_3, R = Me, Et) and found that the NO rotational distributions were insensitive to the size of the substituted ligands.[21] These results revealed that the energy does not flow through all of the vibrational modes in the molecule

before the Co−NO bond breaks. For the molecules studied here, the higher NO rotational population from the photolysis of $Mn(CO)_4NO$ shows that there is more available energy to the NO fragment in the Mn−NO case, relative to the Co−NO case, assuming the exit channels have similar shapes. Following a prompt dissociation of the M−NO bond, as suggested by Georgiou and Wight's results, dissociating the Mn-containing compound produces NO with a higher rotational excitation, which reveals the energy differences between Co−NO and Mn−NO bond dissociation energies. Since the BDEs of neutral metal nitrosyls are not well understood, the closest comparison would be with metal−carbonyl bond energies. The average metal−CO bond dissociation energy in $Mn(CO)_5$ is 20.6 ± 0.6 kcal/mol and in $Co(CO)_4$ is 32 ± 0.8 kcal/mol.[34] The bond dissociation energies for the sequential dissociation of carbonyl ligands vary considerably; for example, dissociating the first carbonyl from $Fe(CO)_5$ takes 41 kcal/mol[35] and dissociating the last carbonyl (from FeCO) takes only 8−10 kcal/mol.[36,37] In general, however, a higher number of d electrons on the metal center stabilizes the back-bonding to π-accepting ligands, such as CO and NO, which increases the metal−ligand BDE. By these arguments, it is reasonable to expect the Co−NO bond to be stronger than Mn−NO, because Co has a d^9 electron configuration and Mn has only a d^7 electron configuration. Such M−NO BDE differences would be apparent in the NO rotational distribution. With more excess energy after the metal−NO bond is broken, the NO distribution would appear hotter in the Mn−NO case.

The central question in these experiments is the role of doubly degenerate orbitals in the dissociation of organometallic nitrosyl compounds. In $Co(CO)_3NO$, the MLCT transition involves excitation of an electron from an orbital of *a* symmetry primarily on the metal to one of two degenerate ligand-based orbitals of *e* symmetry.[23] The excited molecule is expected to undergo a Jahn−Teller distortion to remove the degeneracy of the now nonequivalent orbitals. In $Mn(CO)_4NO$, MLCT involves excitation of an electron from a ground-state orbital of *a* symmetry to an excited-state orbital of *b* symmetry that is nondegenerate. There should be no impulse for a Jahn−Teller distortion. The qualitative shapes of the Boltzmann plots in Figure 5 give little indication of a significant difference in excited-state geometry between $Co(CO)_3NO$ and $Mn(CO)_4NO$ prior to dissociation. There are several plausible explanations of the similar photodissociation behavior seen in these two compounds despite the differences that are predicted from simple electronic structure arguments.

The first explanation for the similar behavior is that neither compound may undergo Jahn−Teller distortion. Barckholtz and Miller have shown that in gas-phase C_{3v} molecules, impulses for Jahn−Teller distortions are counteracted by spin−orbit coupling.[38] In $Co(CO)_3NO$ spin−orbit coupling due to the large number of electrons on the metal center could counteract the impulse for the expected Jahn−Teller bending. Thus, $Co(CO)_3NO$ would behave like $Mn(CO)_4NO$ in the excited state and neither would undergo impulsive dissociation through a bent transition state. Both compounds would then display similar dynamical behavior in the dissociation of NO.

A second possibility for the similarity of the NO rotational distributions is that excited-state Jahn−Teller distortions may occur in both metal compounds. Transfer of electron density from the metal center to the NO ligand would give each compound the impetus to move the carbonyls toward a planar geometry. In $Co(CO)_3NO$, this retains the C_{3v} geometry about the metal center and, thus, the character of the excited-state orbitals. In $Mn(CO)_4NO$, however, this distortion would push the compound toward C_{4v} geometry, where the two excited-state orbitals of *b* symmetry would become a set of degenerate orbitals with *e* symmetry. In that situation, MLCT excitation would induce the Mn−NO bond to bend in a Jahn−Teller distortion, splitting the degeneracy of the singly occupied orbital and the empty orbital. This argument is supported by the data of Crichton and Rest, who excited $Mn(CO)_4NO$ and observed a reduced frequency for ν(NO), arising from a metal-to-nitrosyl charge transfer.[18] In the same experiment they also found that two new CO stretching frequencies grew along with the new ν(NO), an observation that would be expected if a C_{4v} geometry formed in excited $Mn(CO)_4NO$.

Another explanation of the similar NO populations for both compounds arises from a question of the gas-phase geometry of $Mn(CO)_4NO$. Most textbooks and review articles assign the geometry of $Mn(CO)_4NO$ based on a −110 °C crystal structure, where NO is in an equatorial position of a trigonal bipyramid as the equilibrium geometry (**2**).[39] Theoretical treatments of the geometry of five-coordinate metal nitrosyl compounds give further justification for the preference of the NO for the equatorial position of the trigonal bipyrimdal geometry.[40] A high-resolution gas-phase IR study of $Mn(CO)_4NO$, however, has assigned the room-temperature gas-phase geometry of $Mn(CO)_4NO$ to a C_{3v} geometry (**3**) in which the NO is in an axial position.[41] Because there is only modest cooling in the neat molecular beam employed in this study, $Mn(CO)_4NO$ may have the NO group in the equatorial position, in a C_{2v} geometry, or have sufficient internal energy for the molecule to be in equilibrium between the two structures, C_{2v} and C_{3v}, through a Berry pseudorotation.[42] Then there would be similar orbital interactions for both C_{3v} $Co(CO)_3NO$ and C_{3v} $Mn(CO)_4NO$, leading to similar dynamical behavior.

Finally, the rotational distributions of the photodissociated NO may be similar because both molecules rapidly relax to the ground-state electronic surface, in which both have linear M−NO geometries, through which they dissociate. Each would dissociate on a potential surface with a linear equilibrium geometry.

Why is there is significant difference between Georgiou and Wight's one-color REMPI experiments[21,22] and the two-color pump−probe experiments reported here? One explanation could be the 100 ns time delay between pump and probe in our experiments. Predissociative molecules may not have sufficient time to fall apart in a 10 ns 450 nm laser pulse, and thus we would see a different rotational distribution with a 100 ns delay between pump and probe than Georgiou and Wight, who performed excitation and detection in the same laser pulse. We attempted one-color photodissociation and LIF in a single 450 nm laser pulse with $Mn(CO)_4NO$. Because of the increased spectral congestion from the addition of O and S branches to the NO LIF spectrum, as well as low signal-to-noise, no state-resolved information could be determined from these experiments. One-color photodissociation/LIF experiments with $Co(CO)_3NO$ were not attempted.

V. Conclusions

Two metal nitrosyl compounds, $Co(CO)_3NO$ and $Mn(CO)_4NO$, were photodissociated at 450 nm, in the metal-to-ligand charge-transfer region for both compounds. Free NO was detected by laser-induced fluorescence excitation to determine the rotational distribution of the nascent NO products in the $v'' = 0$ vibrational state. The highest assigned rotational state gives an upper limit to the Co−NO and Mn−NO bond

dissociation energies at 52 kcal/mol. The NO product distribution was compared to the Prior Distribution through a Surprisal Analysis. The NO population distribution displays a dynamical bias toward lower rotation in both compounds. The similarity of the NO rotational distributions is surprising, considering that $Co(CO)_3NO$ was expected to undergo a Jahn−Teller distortion to bend the Co−NO bond in the excited state and $Mn(CO)_4NO$ was not expected to distort. The surprising similarities can be explained by the combined effects of Jahn−Teller and spin−orbit coupling, excited-state distortions of $Mn(CO)_4NO$, a C_{3v} geometry in the ground state of $Mn(CO)_4NO$, or by rapid relaxation to the ground state prior to dissociation in both compounds. The spin−orbit populations of the NO products ($^2\Pi_{1/2}$ and $^2\Pi_{3/2}$) are equally populated in dissociating both compounds, indicating that the electronic surfaces that produce these two states are strongly coupled at the transition state but not influenced by the energy differences in the separated products.

Acknowledgment. This work was supported by the Camille and Henry Dreyfus Foundation through a Start-Up Award for Undergraduate Institutions, a Cottrell College Science Award from Research Corp., and a Research Opportunity Award through the National Science Foundation. S.O. received scholarship support from Nihon University. K.P.B. acknowledges a summer fellowship from the Division of Laser Science of the American Physical Society.

References and Notes

(1) Crawford, N. R. M.; Knutsen, J. S.; Yang, K. A.; Haugstad, G.; McKernan, S.; McCormick, F. B.; Gladfelter, W. L. *Chem. Vap. Deposition* **1998**, *4*, 181.
(2) Lane, P. A.; Oliver, P. E.; Wright, P. J.; Reeves, C. L.; Pitt, A. D.; Cockayne, B. *Chem. Vap. Deposition* **1998**, *4*, 183.
(3) Snyder, S. H.; Bredt, D. S. *Sci. Am.* **1992**, *May*, 68.
(4) Reisler, H.; Noble, M.; Wittig, C. In *Molecular Photodissociation Dynamics*; Ashfold, M. N. R., Baggot, J. E., Eds.; Royal Society of Chemistry: London, 1987.
(5) D'Azy, O. B.; Lahmani, F.; Lardeux, C.; Solgadi, D. *Chem. Phys.* **1985**, *94*, 247.
(6) Lahmani, F.; Lardeux, C.; Solgadi, D. *Chem. Phys. Lett.* **1983**, *102*, 523.
(7) Qian, C. X. W.; Noble, M.; Nadler, I.; Reisler, H.; Wittig, C. *J. Chem. Phys.* **1985**, *83*, 5573.
(8) Hunter, M.; Reid, S. A.; Robie, D. C.; Reisler, H. *J. Chem. Phys.* **1993**, *99*, 1093.
(9) Tomer, J. L.; Wall, M. C.; Reid, B. P.; Cline, J. I. *J. Chem. Phys.* **1995**, *102*, 6100.
(10) Lahmani, F.; Lardeux, C.; Solgadi, D. *Chem. Phys. Lett.* **1986**, *129*, 24.
(11) Bower, R. D.; Jones, R. W.; Houston, P. L. *J. Chem. Phys.* **1983**, *79*, 2799.
(12) Dyet, J. A.; McCoustra, M. R. S.; Pfab, J. *J. Chem. Soc., Faraday Trans.* **1990**, *86*, 2049.
(13) Spasov, J. S.; Cline, J. I. *J. Chem. Phys.* **1999**, *110*, 9568.
(14) Noble, M.; Qian, C. X. W.; Reisler, H.; Wittig, C. *J. Chem. Phys.* **1986**, *85*, 5763.
(15) Castle, K. J.; Abbott, J.; Peng, X.; Kong, W. *Chem. Phys. Lett.* **2000**, *318*, 565.
(16) Crichton, O.; Rest, A. J. *J. Chem. Soc., Dalton Trans.* **1977**, 536.
(17) Keeton, D. P.; Basolo, F. *Inorg. Chim. Acta* **1972**, *6*, 33.
(18) Crichton, O.; Rest, A. J. *J. Chem. Soc., Dalton Trans.* **1978**, 208.
(19) Chen, L. X.; Bowman, M. K.; Wang, Z.; Montano, P. A.; Norris, J. R. *J. Phys. Chem.* **1994**, *98*, 9457.
(20) Evans, W.; Zink, J. I. *J. Am. Chem. Soc.* **1981**, *103*, 2635.
(21) Georgiou, S.; Wight, C. A. *J. Phys. Chem.* **1990**, *94*, 4935.
(22) Georgiou, S.; Wight, C. A. *Chem. Phys. Lett.* **1986**, *132*, 511.
(23) Enemark, J. H.; Feltham, R. D. *Coord. Chem. Rev.* **1974**, *13*, 339.
(24) Job, R.; Rovang, J. *Synth. React. Inorg. Metal-Org. Chem.* **1976**, *6*, 367.
(25) Treichel, P. M.; Pitcher, E.; King, R. B.; Stone, F. G. A. *J. Am. Chem. Soc.* **1961**, *83*, 2593.
(26) Mallard, W. G.; Miller, J. H.; Smity, K. C. *J. Chem. Phys.* **1982**, *76*, 3483.
(27) Earls, L. T. *Phys. Rev.* **1935**, *48*, 423.
(28) Bartz, J. A.; Friday, T. O.; Goodman, B. R.; Kooi, S. E.; Blair, R. G.; Polik, W. F. *J. Phys. Chem. A* **1998**, *102*, 10697.
(29) Georgiou, S.; Wight, C. A. *J. Chem. Phys.* **1988**, *88*, 7418.
(30) Georgiou, S.; Wight, C. A. *J. Chem. Phys.* **1989**, *90*, 1694.
(31) Bartz, J. A.; Burke, K. P.; Cekola, J. J.; Leroi, G. E. Manuscript in preparation.
(32) Hellner, L.; Masanet, J.; Vermeil, C. *Chem. Phys. Lett.* **1981**, *83*, 474.
(33) Levine, R. D.; Bernstein, R. B. *Molecular Reaction Dynamics and Chemical Reactivity*; Oxford: New York, 1987.
(34) Sunderlin, L. S.; Weng, D.; Squires, R. R. *J. Am. Chem. Soc.* **1993**, *115*, 12060.
(35) Lewis, K. E.; Golden, D. M.; Smith, G. P. *J. Am. Chem. Soc.* **1984**, *106*, 3905.
(36) Sunderlin, L. S.; Wang, D.; Squires, R. R. *J. Am. Chem. Soc.* **1992**, *114*, 2788.
(37) Villalta, P. W.; Leopold, D. G. *J. Chem. Phys.* **1993**, *98*, 7730.
(38) Barckholtz, T. A.; Miller, T. A. *Int. Rev. Phys. Chem.* **1998**, *17*, 435.
(39) Richter-Addo, G. B.; Legzdins, P. *Metal Nitrosyls*; Oxford: New York, 1992.
(40) Hoffmann, R.; Chen, M. M. L.; Elian, M.; Rossi, A. R.; Mingos, D. M. P. *Inorg. Chem.* **1974**, *13*, 2666.
(41) Barna, G.; Butler, I. S. *Can. J. Spectrosc.* **1972**, *17*, 2.
(42) Berry, R. S. *J. Chem. Phys.* **1960**, *32*, 933.